

# Evaluation of Additively Manufactured Candidate Alloys for Hydrogen Turbine Fuel Injectors

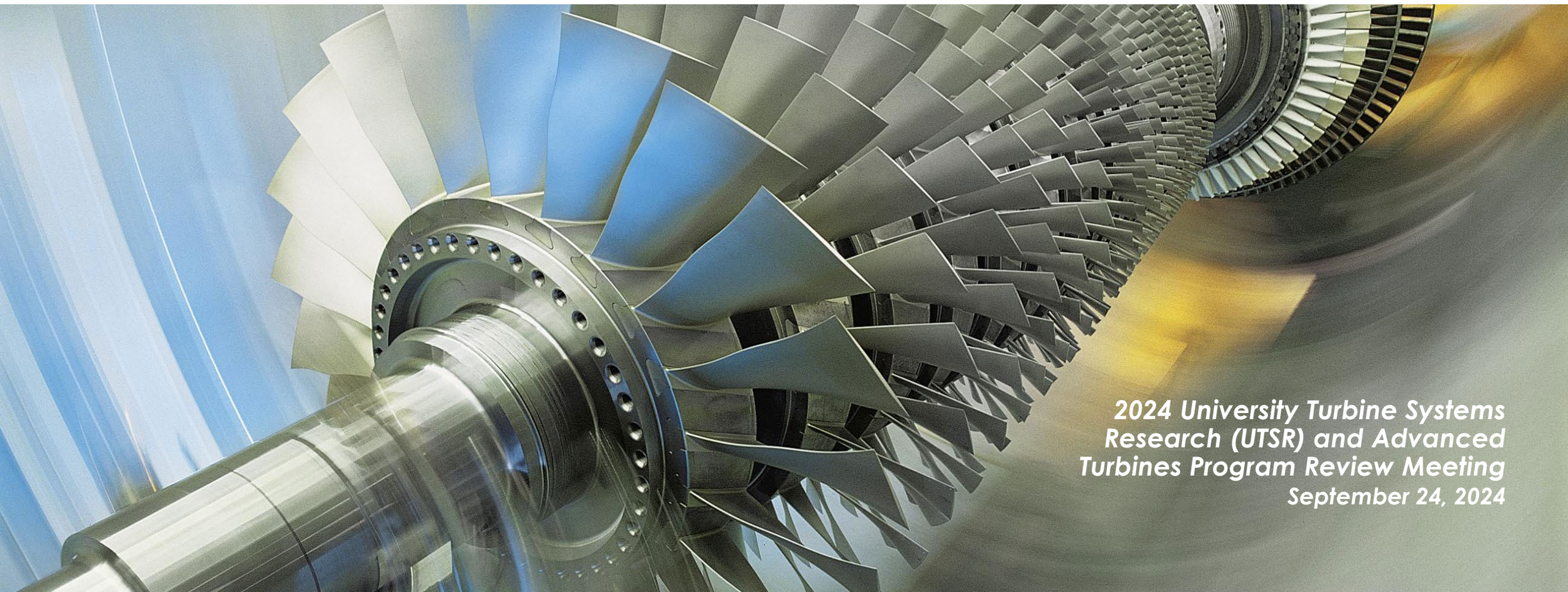


**PI: Chantal Sudbrack\* Rui Feng, Kyle Rozman, Lucas Teeter, Yoosuf Picard, Martin Detrois**

*\* Structural Materials Team  
Materials Engineering & Manufacturing Directorate  
Research and Innovation Center  
chantal.sudbrack@netl.doe.gov*

**Presenter: David Alman**

*Materials Engineering & Manufacturing Directorate  
Research and Innovation Center; david.alman@netl.doe.gov*



*2024 University Turbine Systems  
Research (UTSR) and Advanced  
Turbines Program Review Meeting  
September 24, 2024*

# Acknowledgements



This research was conducted in support of the DOE FECM/NETL Hydrogen with Carbon Management Advanced Turbines Program, **Robert Schrecengost, DOE-FECM Division Director, John Crane, NETL Technology Manager**, and executed through Goal 4 of NETL Research & Innovation Center's Advanced Turbine MYRP, **Nathan Weiland**, MYRP lead, **Peter Strakey** Technology Portfolio Lead.

**Siemens: Anand Kulkarni and Ramesh Subramanian**

**NETL: Ritam Pal** for fractography and ANSYS simulations (ORISE PIP Intern) for fractography and ANSYS simulations; **Peter Strakey** for injector face FEA modeling; **Ömer Doğan, Kaimiao Liu, and Kristin Tippey** for useful discussions; **Chris Powell and Devin Hlvanika** for mechanical testing; **Richard Chinn and Chris McCaig** for LECO/WXRF analysis. **Dennis Harvey** for metallographic preparation; **Trevor Godell** for test bar machining. **Thomas Kalapos** for project management support.

**Disclaimer:** Neither the United States Government nor any agency thereof, nor any of their employees, nor the support contractor, nor any of their employees, makes any warranty, express or implied, or assumes any legal liability or responsibility for the accuracy, completeness, or usefulness of any information, apparatus, product, or process disclosed, or represents that its use would not infringe privately owned rights. Reference herein to any specific commercial product, process, or service by trade name, trademark, manufacturer, or otherwise does not necessarily constitute or imply its endorsement, recommendation, or favoring by the United States Government or any agency thereof. The views and opinions of authors expressed herein do not necessarily state or reflect those of the United States Government or any agency thereof.

Some of these projects were funded by the United States Department of Energy, National Energy Technology Laboratory, in part, through a site support contract.

# Motivation & Approach

**Hydrogen turbine technology:** Hydrogen and hydrogen/natural gas blends are being pursued to reduce emissions and improve engine operating efficiency

**Laser powder bed fusion (L-PBF) fabrication:** Design of fuel injectors with cooling passages & fuel channels for both premixed and non-premixed gas turbine combustion systems

**Goal: Document AM candidates in operation ranges that are undocumented and relevant to hydrogen service**

**Approach:** Property-Microstructure Evaluation L-PBF Ni-Superalloy for Industrial Gas Turbine Fuel Injectors

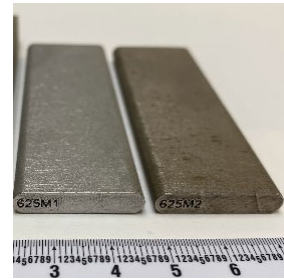
- Alloys: Solid Solution (IN625),  $\gamma'$  Precipitate (Haynes 230),  $\gamma'/\gamma''/\delta$  Precipitate (IN 718) strengthen
- Compare L-PBF properties to wrought properties
- Screen the **tensile, creep, and fatigue** properties up to 815 °C in air.
  - Porosity / defects - Location specific microstructure – Impact of minor phases
  - Failure mechanisms with fractography, cross-section analysis, and TEM
- **Assess hydrogen embrittlement (HE) susceptibility** using slow strain-rate tensile testing
  - Ex-situ electrochemically charged and then test to failure
  - Extend to in-situ testing, examine elevated temperature hydrogen attack and damage
- Screen materials behavior under conditions that mimic service
  - Coupon exposure various fuel environments at elevated temperature, pressure, and H<sub>2</sub>O vapor
  - Capture prior thermal history & assess impact on select properties

On-going  
& future  
work

# Laser Powder Bed Fusion (L-PBF) Processing

- IN625, IN718, Haynes 282
- **L-PBF printing with Ar gas-atomized powders**
  - Siemens
  - **EOS M290 machine**
- Optimized parameters consistent with EOS specifications,
- Bidirectional scan strategy
- 40  $\mu\text{m}$  layer thickness
- Vertical Z-direction test bars and blanks in the build direction
- Stress Relief on the build plate
- Heat treated to industrial practice.

(1) Met. as-printed  
(1) Met. solutioned



(5) Tensile / Creep  
Z-blanks



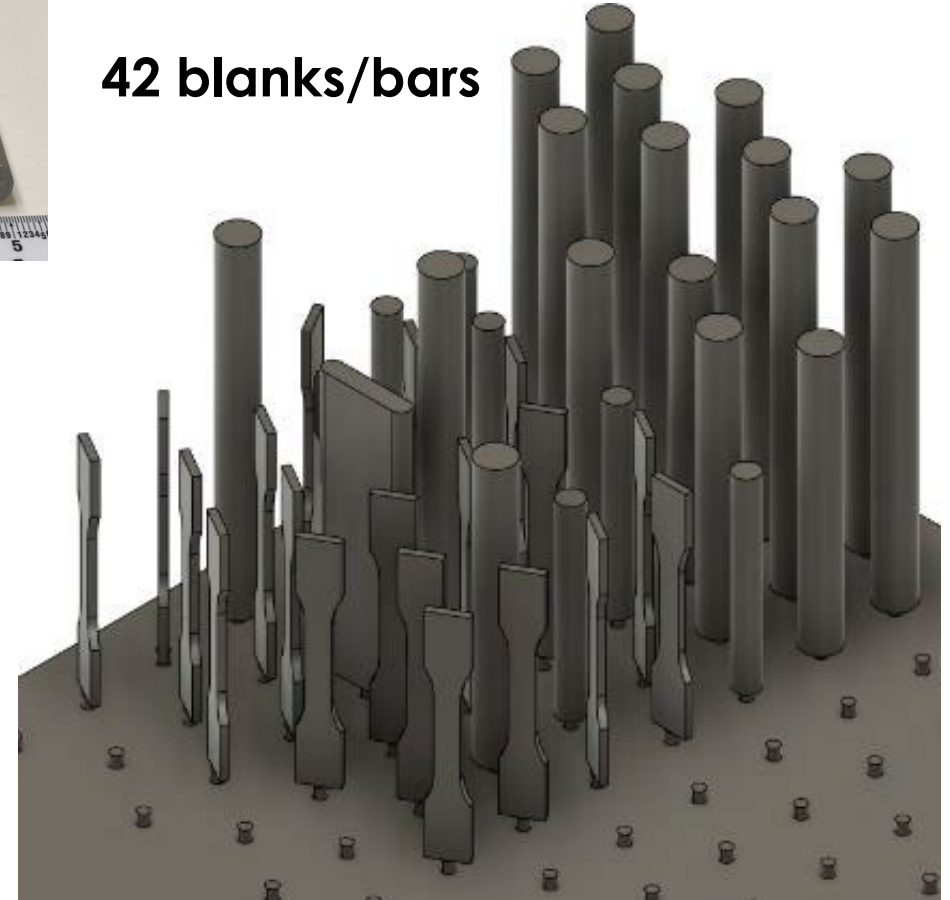
(13) Oversized Z-blanks



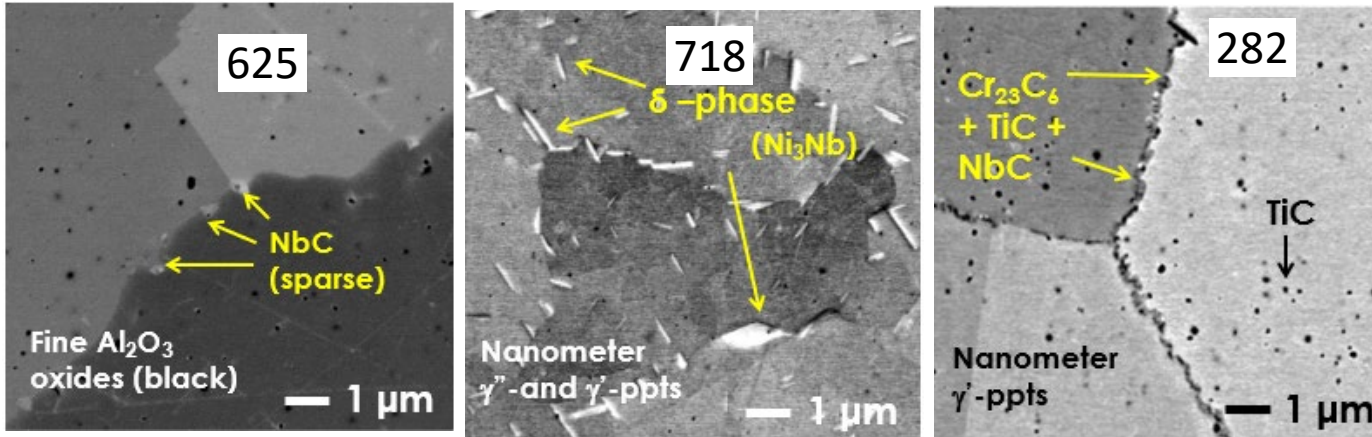
(20) Z-dog bones HE Tests



42 blanks/bars



## Solid Solution vs. $\gamma'/\gamma''/\delta$ Precipitate vs. $\gamma'$ Precipitate Strengthen



### Heat Treatment:

- Stress-relieved on the build plate
- **L-PBF 625 (no HIP)**: Solution heat treatment at 1175 °C for 1 hour. As-printed porosity measured to be 0.04 + 0.02 % → **HIP does not appear necessary**
- **L-PBF 718 (w/HIP)**: Modified AMS 5663 specification schedule. Solutioning at ~980 °C for 1 hour (**below  $\delta$ -solvus**) + similar holds/temps for 2-step aging
- **L-PBF 282 (w/HIP)**: Two-step solutioning above 1150 °C with 1 hour holds each. Standard single step aging 788 °C for 8 hours

## WDXRF/LECO Measured Compositions on L-PBF Material

Wt.%	Ni	Cr	Mo	Nb	Fe	Ti	Al	Co	C
L-PBF 625	61.5	21.3	9.1	3.7	4.0	0.08	0.06	0.08	0.0124
L-PBF 718	52.9	18.7	3.1	5.16	18.3	0.96	0.48	0.21	0.0525
L-PBF H282	58.1	19.2	8.8	0.05	0.11	2.12	1.22	10.3	0.0459

## Composition Compared to Specifications

Carbon specification

Wt.%	C
<b>625</b>	<b>0.10 max</b>
<b>718</b>	<b>0.08 max</b>
<b>H282</b>	<b>0.06</b>

Low C content L-PBF 625 →

Alloy specifications

<https://www.specialmetals.com/documents/technical-bulletins/inconel/inconel-alloy-718.pdf>

<https://www.specialmetals.com/documents/technical-bulletins/inconel/inconel-alloy-625.pdf>

<https://haynesintl.com/en/datasheet/haynes-282-alloy/#alloy-brochuref>

# Grain structure after heat treatment

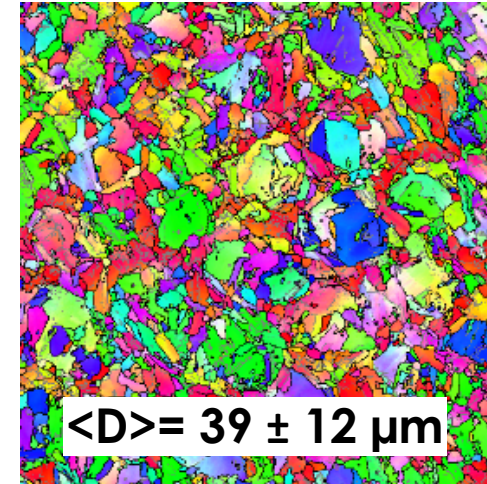
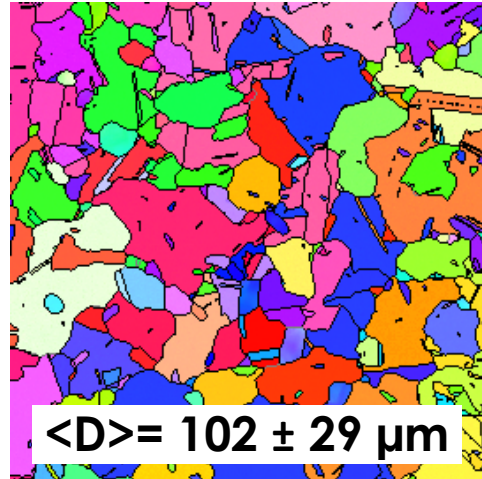
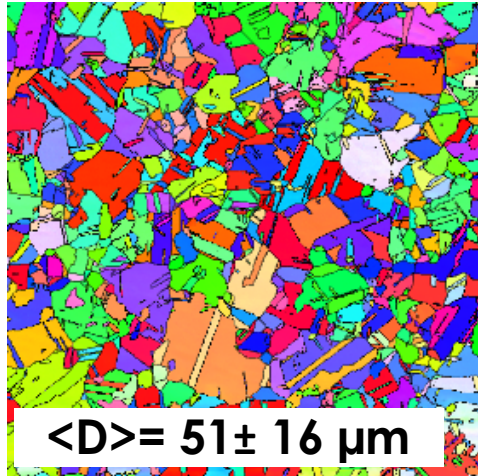
Near equiaxed: *Grains recrystallize*

625

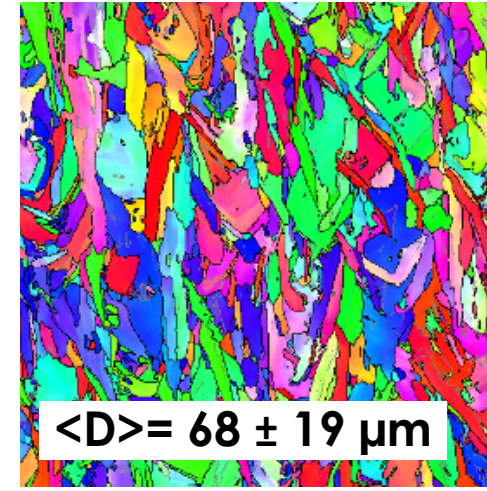
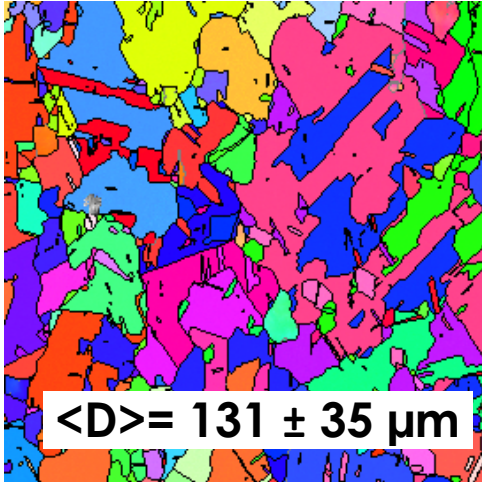
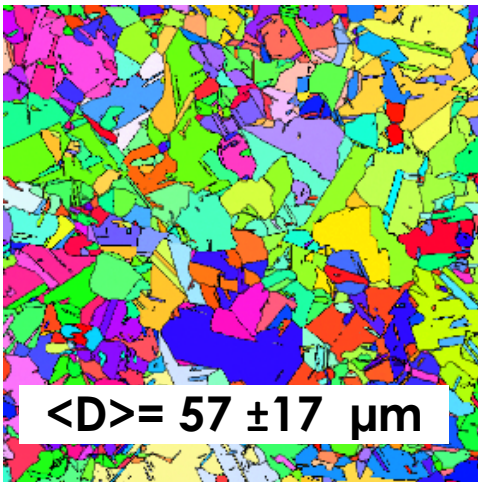
282

718

In-Plane  
(XY)

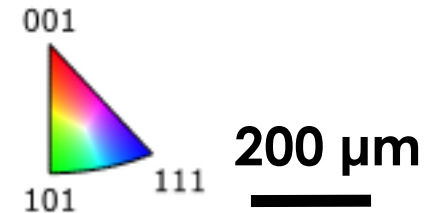


Along Build  
Direction  
(XZ)



Elongated like  
As-printed:

*Grains  
restrained by  
 $\delta$ -ppts at GBs*



# Mechanical Tests

## L-PBF 625, 718, 282 property tested in fully heat-treated condition

### Three tensile tests (E8/E21)

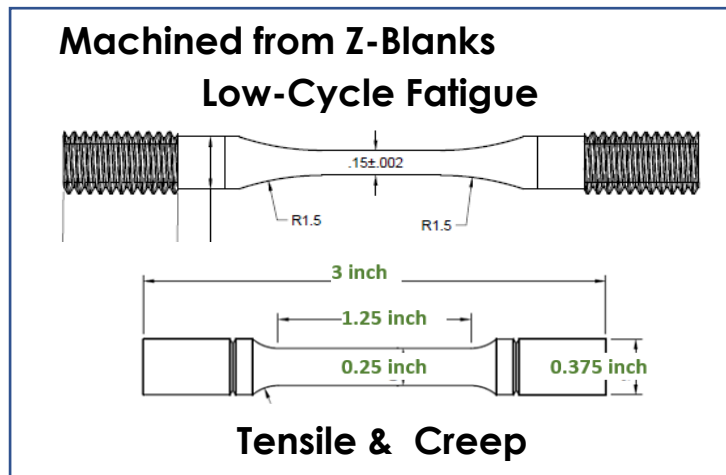
- **Room Temp, 650°C, 750°C**
- 1 test each at  $2.17 \times 10^{-3}$  mm/s to 1.2%, then  $2.17 \times 10^{-2}$  mm/s thereafter

### Four creep rupture tests (E139)

- 650 – 815 °C / 100 – 600 MPa

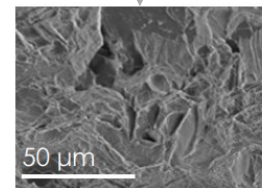
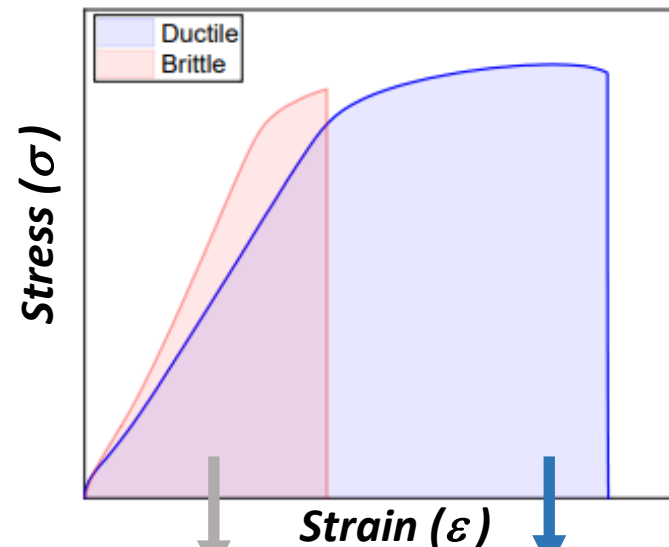
### Eleven strain-controlled low cycle-fatigue tests

- 650 °C
- Strain range vs. Fatigue Life ( $N_f$ ) curve (S-N curve)
- R= 0.05, f= 0.2 Hz for strain range up to 1.5%

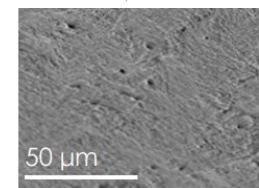


### Hydrogen embrittlement – 5 slow strain tensile tests at RT

- Surfaces milled to 600 grit finish - good electrical contact for charging.
- **Ex-situ H<sub>2</sub> charging** at 1 mA/cm<sup>2</sup> in 0.1 M H<sub>2</sub>SO<sub>4</sub> with +1 g/L CH<sub>4</sub>N<sub>2</sub>S for 72 h
- Test to failure using  $6.3 \times 10^{-6} \text{ s}^{-1}$  strain rate



Brittle fracture



Ductile fracture

$$HE_{index} = \frac{\epsilon_{AR} - \epsilon_{HE}}{\epsilon_{AR}}$$

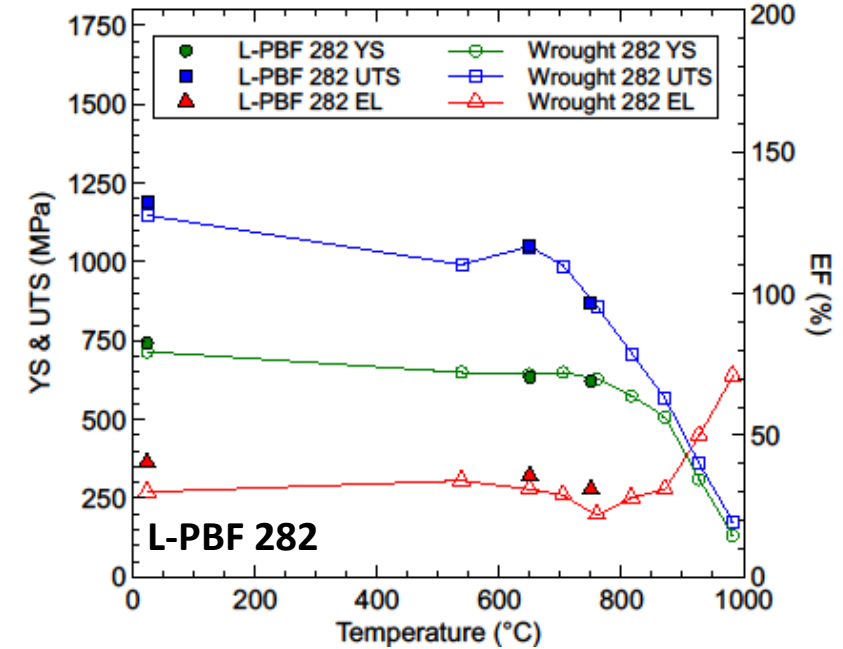
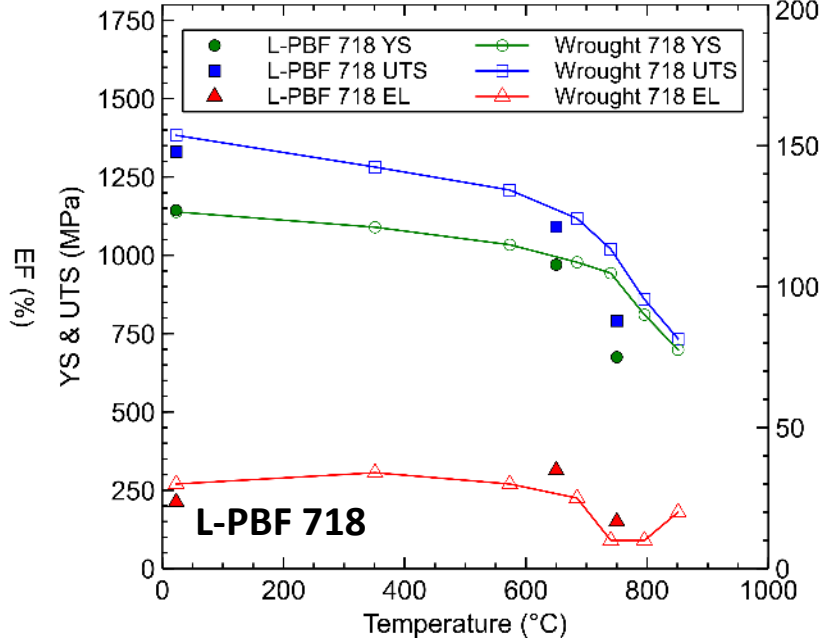
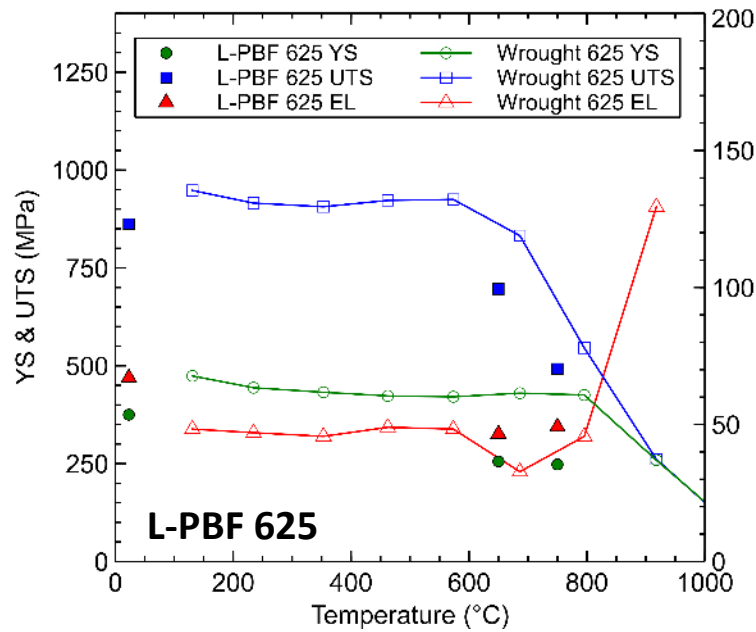
AR = As-received condition (no charging)  
HE = Charged condition

### Near-net shape Z-dog bones



# Tensile Properties

## Room temperature, 650 °C, and 750 °C



## Compared to wrought product:

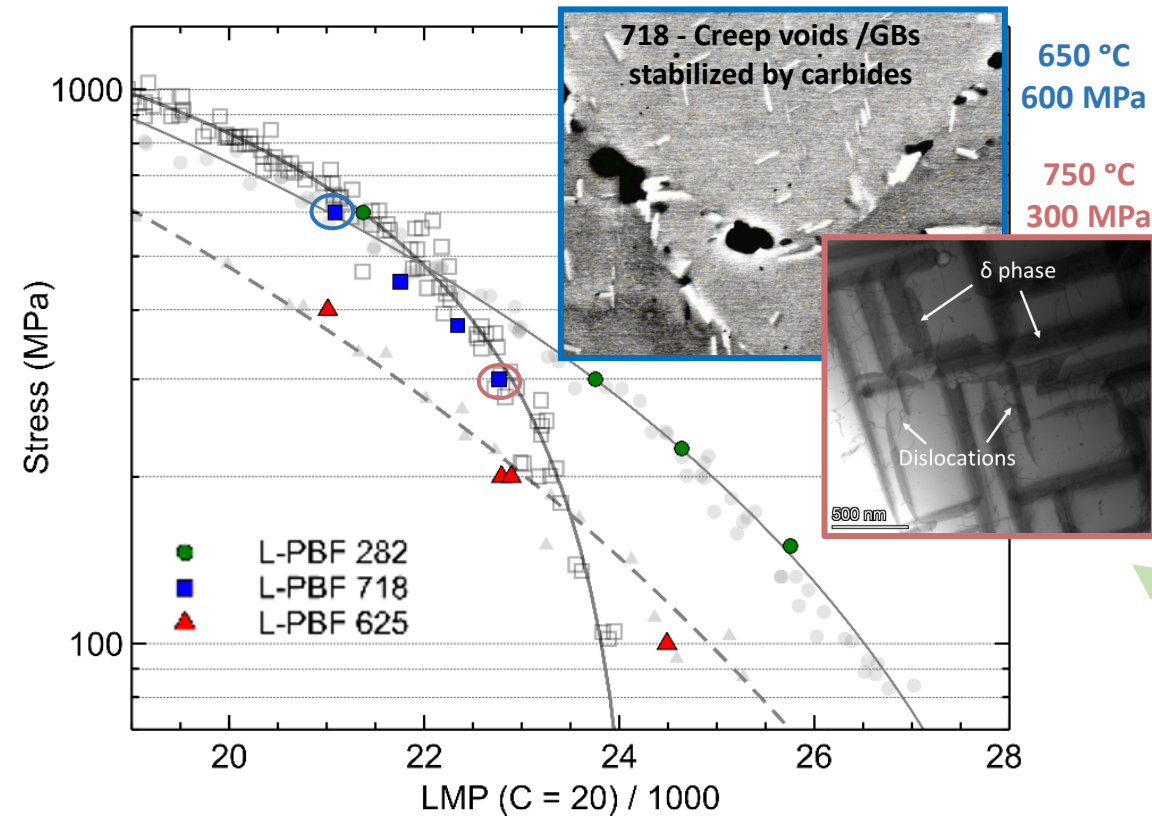
- All L-PBF alloys shows modestly **higher ductilities** over the temperature range
- L-PBF 625/718 Drop-off in **UTS** shifted to lower temperatures by ~50 °C ← **refined grain structures**
- L-PBF 625 **yield strength** significantly lower, possibly due to 124 ppm C content → **fewer MC carbides**
- L-PBF 282 has very comparable **UTS** and **yield-strength** ← **similar grain structure to wrought**



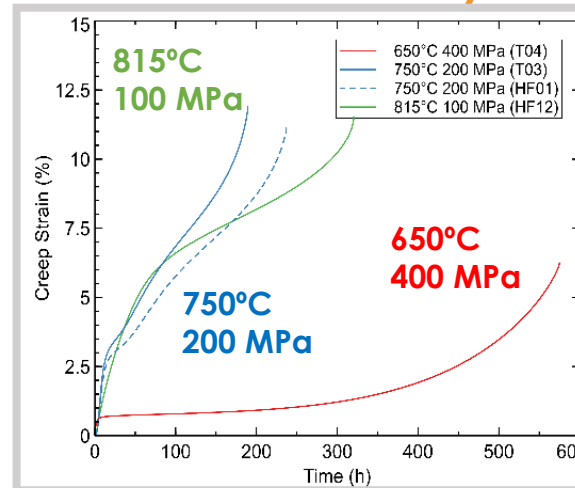
# Creep Behavior

Investigation of deformation behavior and failure modes is underway

## Larson-Miller Plot: All Alloys Compared

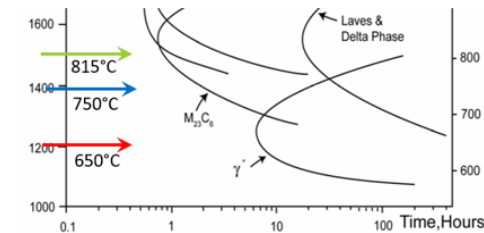


- All three alloys perform like wrought product
- L-PBF 718 is within statistical deviation; however, on the lower side → likely a result of fine, restrained grains

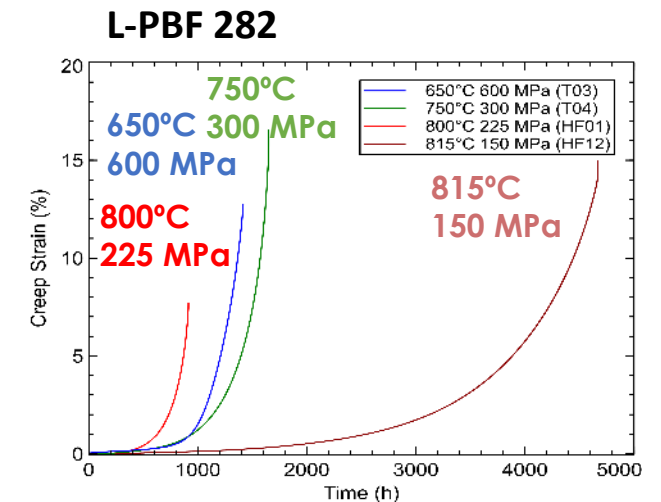
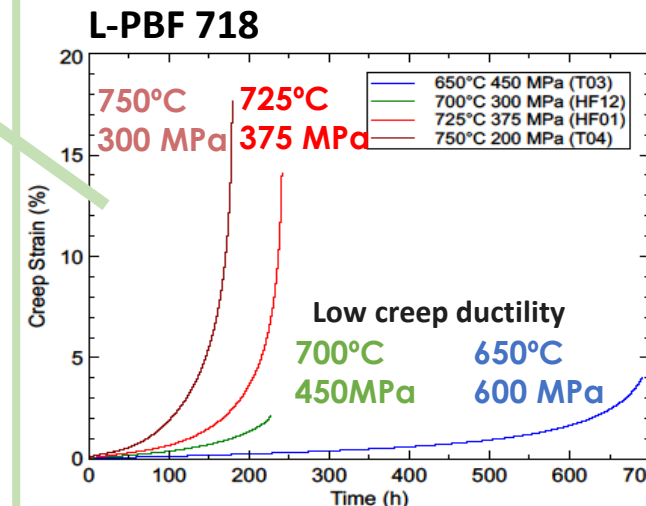


- Double minima for 750°C and 815°C creep curves
  - 1<sup>st</sup> minimum  $\gamma''$  emerges
  - 2<sup>nd</sup> minimum  $\delta$  emerges

L-PBF 625



Well-defined primary, secondary and tertiary stages



# Strain-Controlled Low Cycle-Fatigue

Detail examination of fracture surfaces complete; microstructural linkage and evaluation of hysteresis planned

## Similar performance to wrought alloys

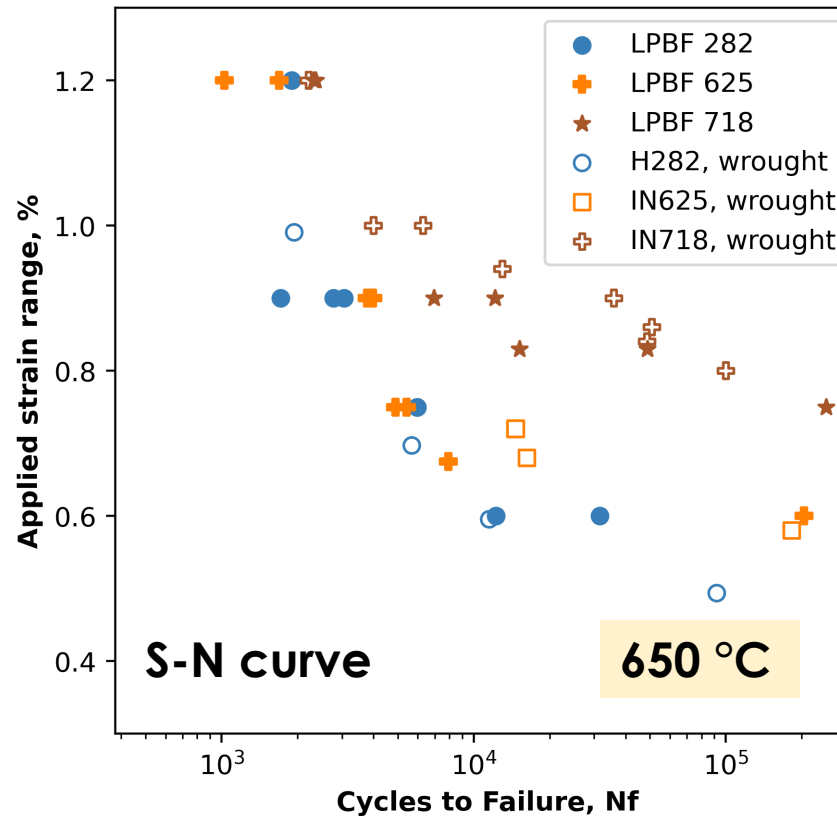
- L-PBF 718 somewhat lower

## For L-PBF 625

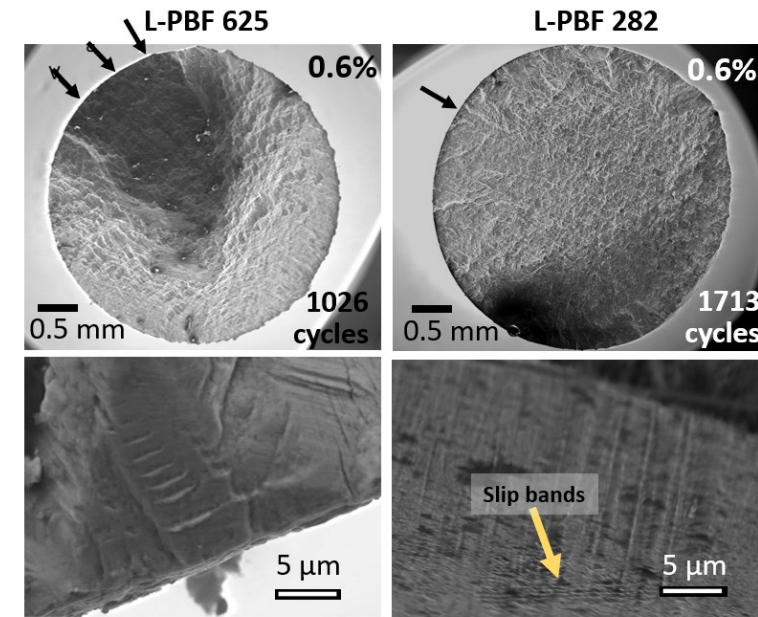
- Low applied strain ranges show stage one crystallographic initiation
- High applied strain ranges show initiations at dislocation egress from the surface

Further work on other alloys and hysteresis underway

### L-PBF (R= 0.05) vs Wrought (R = -1)



### Crack initiation and propagation

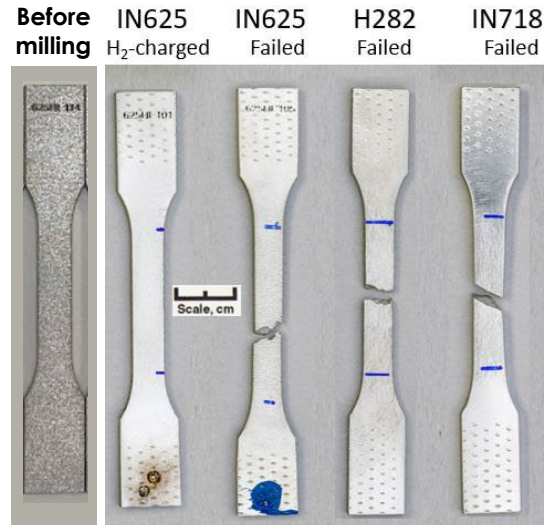


# Slow strain-rate testing to screen H<sub>2</sub>-embrittlement (HE)

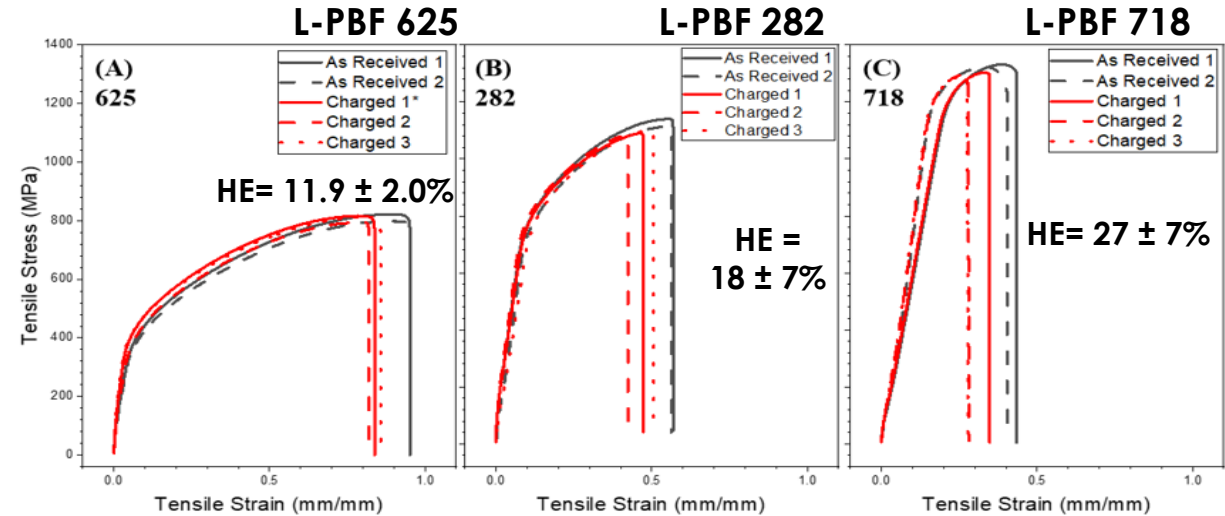
2 Tests on Uncharged / 3 Tests on Charged Test Bars

## Ex-situ H<sub>2</sub> charging

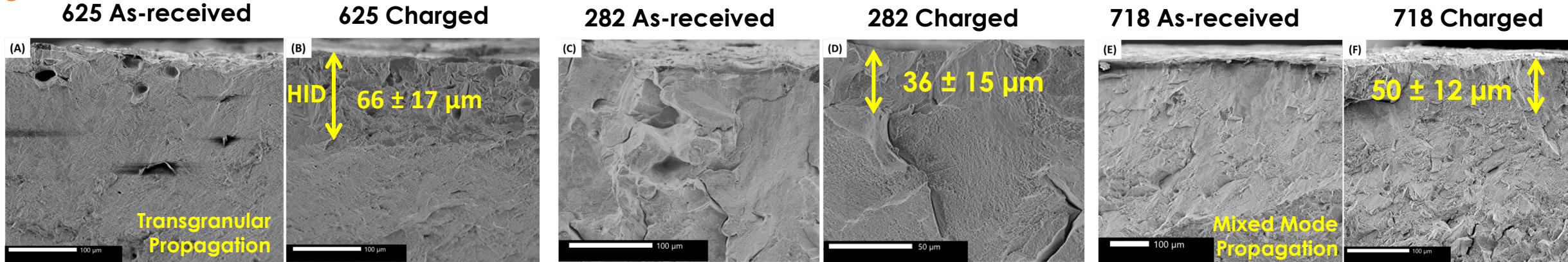
- Largest hydrogen ingress depth (HID) for L-PBF 625
- Brittle features in HID for all three alloys
- Brittle cleavage extends past HID in L-PBF 718



**HE Index**  
L-PBF 718 (most HE) > 282 > 625 (least HE)



## Edge of fracture surfaces:

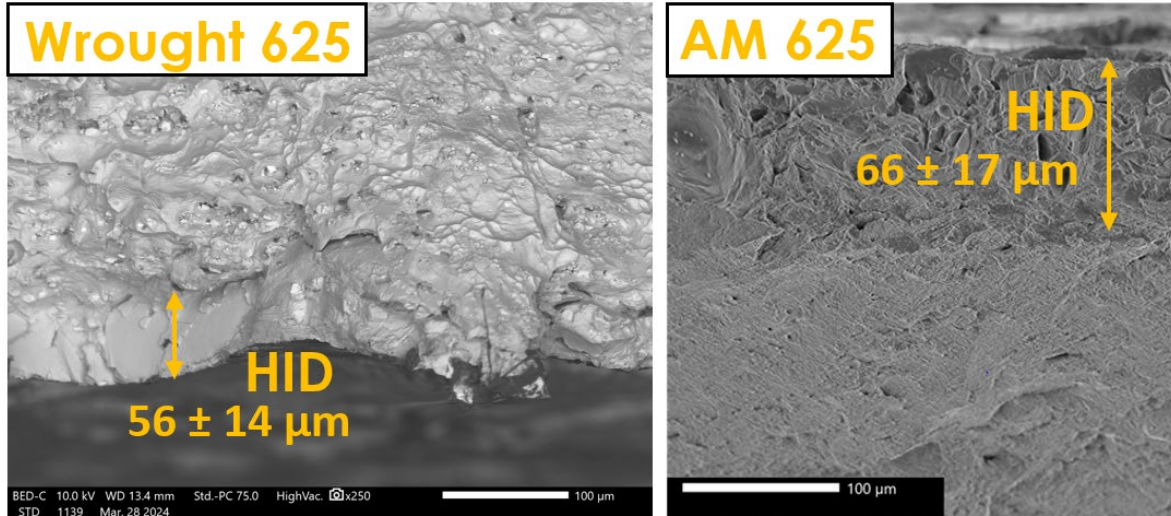


← Recrystallized grains after FHT → ← Restrained grains →

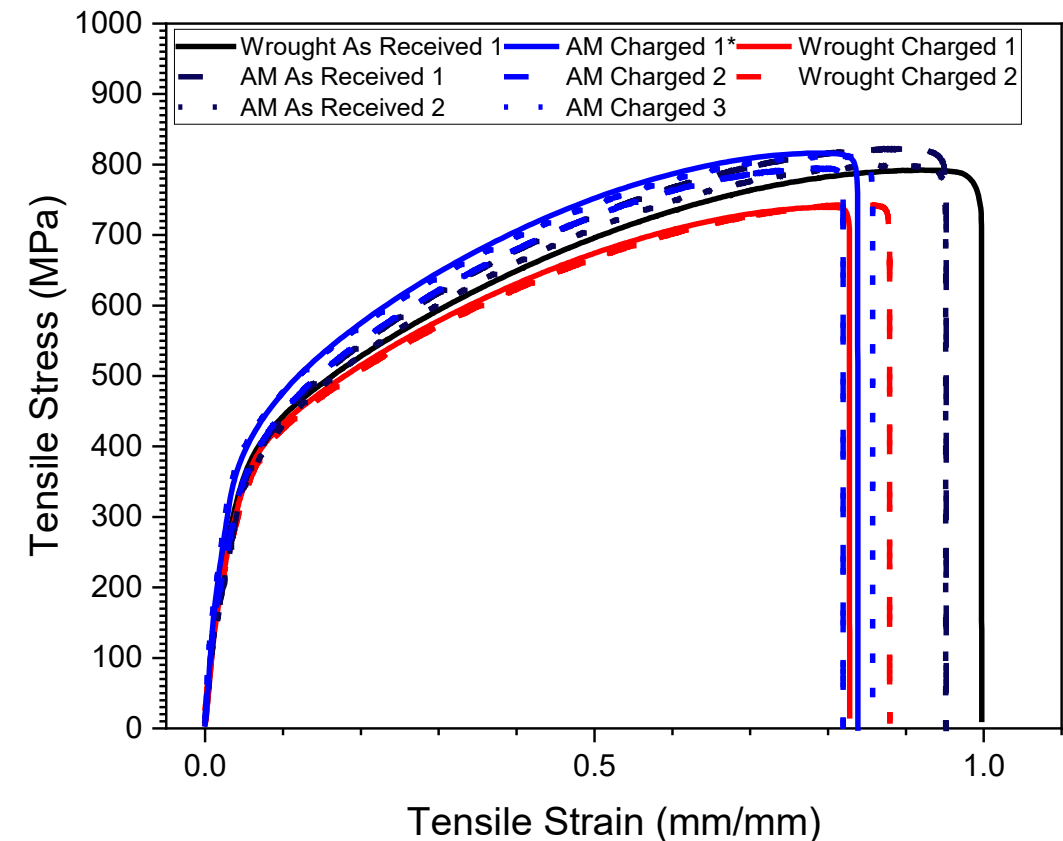
# Wrought Alloy Comparison

## Hydrogen Embrittlement and Fractography

- AM and wrought behavior is similar; however, AM 625 does seem to experience slightly reduced mechanical degradation in comparison to the wrought 625.
- Brittle features on both samples inside HID. HID slightly larger for AM 625



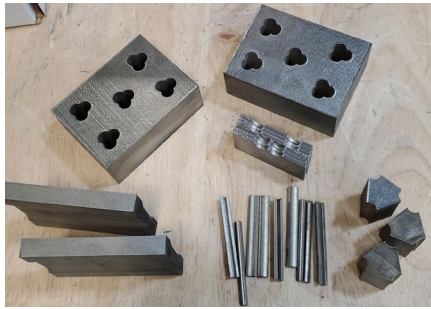
Material	HE Index
Wrought IN625	14.4% ± 3.7%
AM IN625	11.9% ± 2.0%



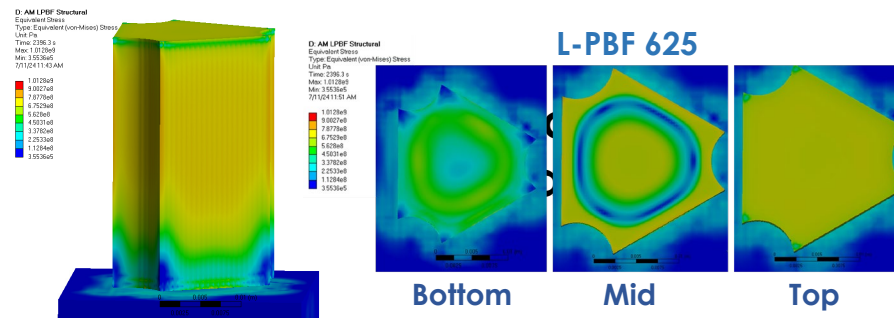
# Geometric Stress Concentration Effect on AM Parts Performance

**Objective:** Understand the effect of geometric residual stress on the materials-hydrogen interactions and performance of fuel injector candidates

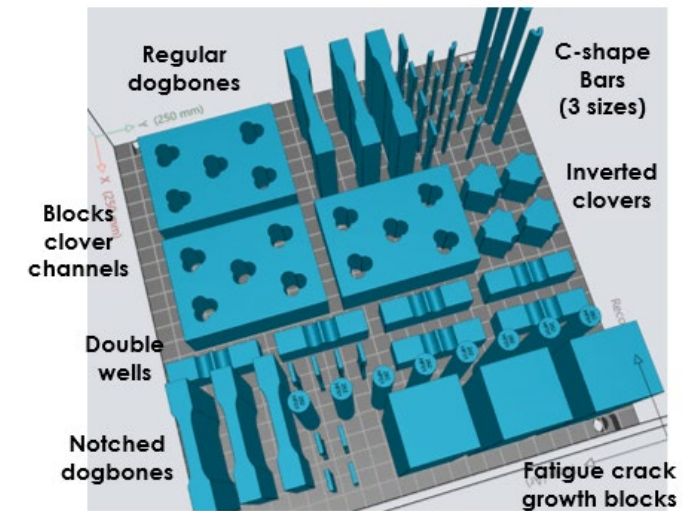
## First Build Set Delivered



## Initial predictions of residual stress distribution



Lab-scale articles that capture realistic injector features: 54 pieces per alloy



## Highlights:

- ✓ **Continued printing partnership** with Siemens Energy
- ✓ **Designed lab-scale articles** with realistic injector geometric features **and completed printing of first alloy**, L-PBF 625
- ✓ **Completed initial residual stress simulations with ANSYS** of select lab-scale articles
- ✓ **Successfully awarded beam time** under am ORNL Neutron Sciences General User Proposal to measure residual stress using Spallation Neutron Scattering (SNS)

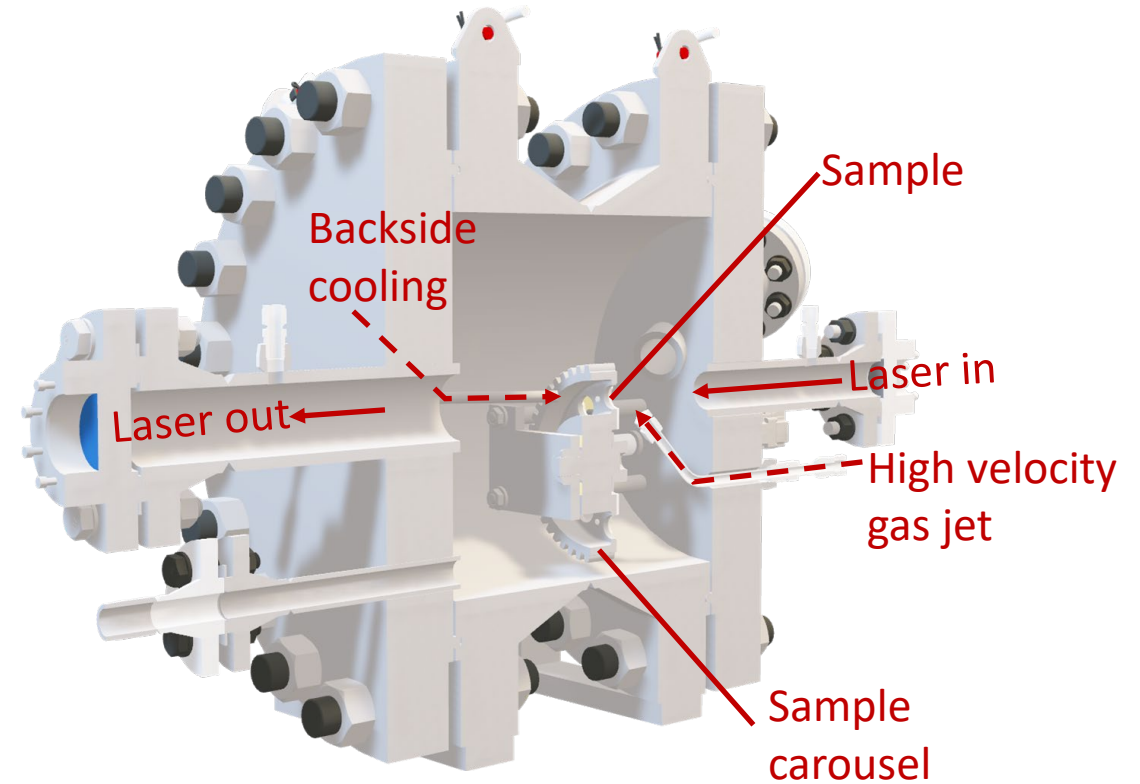
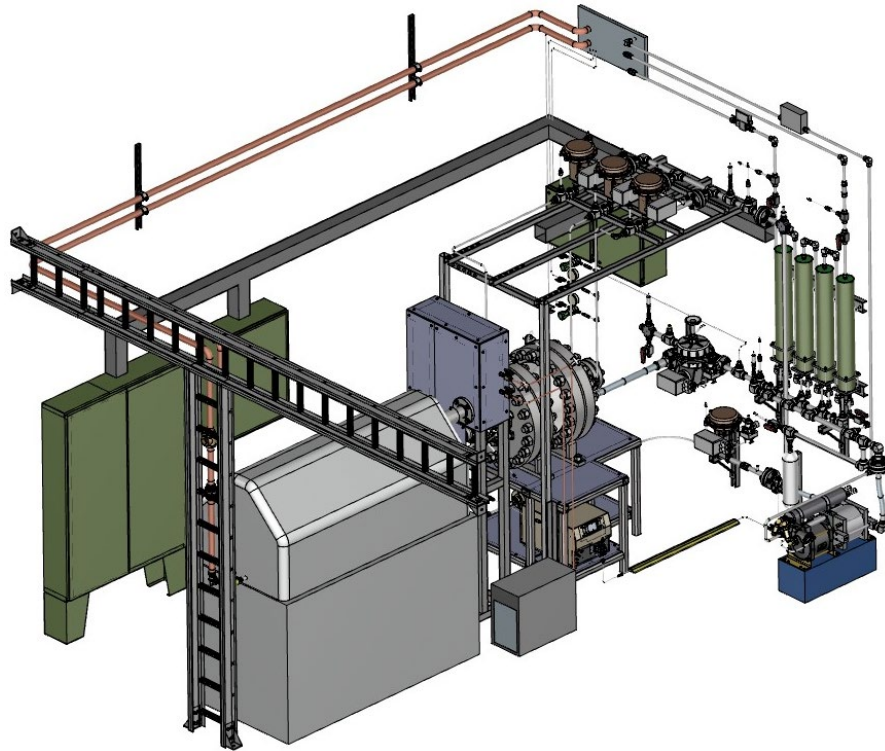
## Next steps:

- **Measure location-specific residual stress of selected geometries using neutron scattering**
- **Assess the impact of stress concentration on H<sub>2</sub>-damage and performance debits**

# Gas Turbine Combustion Simulation Rig

## NETL-Research and Innovation Capabilities

Environmental performance testing of T/EBCs, CMCs, and other high temperature materials



- ✓ Ultrahigh surface temperatures
- ✓ High gas velocity
- ✓ High pressure
- ✓ Complex gas mixtures
- ✓ Backside cooling (thermal gradient)
- ✓ Long exposure times (unattended operations)



**Realistic gas turbine environments**

# Materials Performance in H<sub>2</sub>

## NETL-Research and Innovation Capabilities

### • Fatigue Crack Growth

- Tests can be performed in aqueous electrolyte or in pure hydrogen gas
- Autoclave pressures up to 1500 psi
- Autoclave temperatures up to 288°C

### • Slow strain rate testing

- In-situ (loading while charging)

### • Creep Testing

- Ar-2.8% H<sub>2</sub> Up to 1200°C
- 100% H<sub>2</sub> future

### • Hydrogen autoclave for gaseous pre-charging

- H<sub>2</sub> (pure) (600 °C / 1600 psi)

### • Hydrogen Permeation

- Devanathan – Stachurski cell
- Hydrogen gas permeation

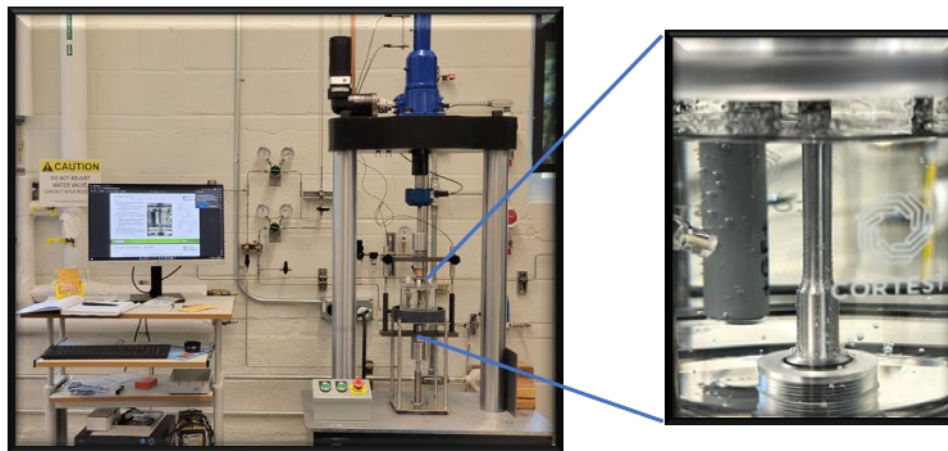
### • Hydrogen absorption / desorption

- Scanning Electrochemical Microscopy

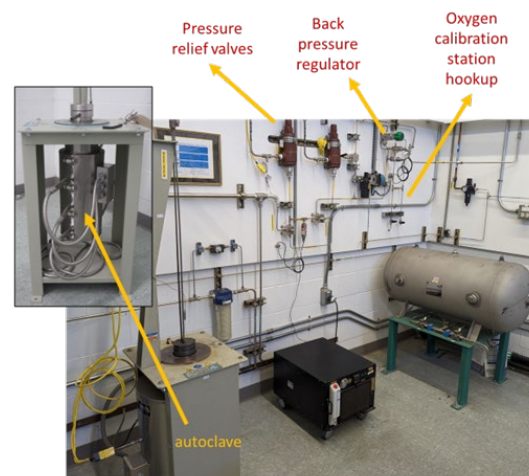
### • Analytical Capabilities

- Thermal Desorption Mass Spectrometry
- Hydrogen microprinting

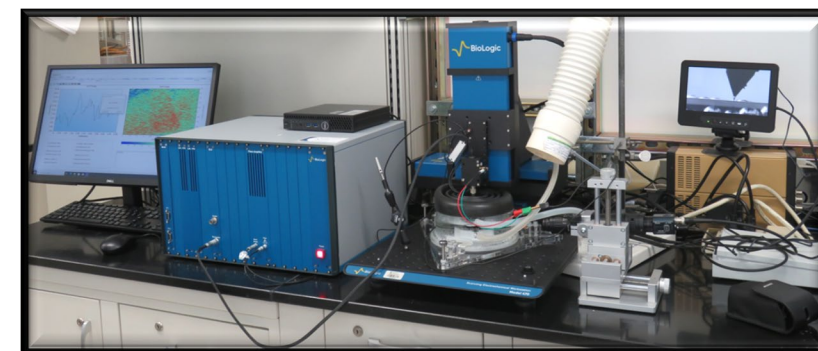
Slow Strain Rate Testing



Fatigue Crack Growth



Hydrogen autoclave for pre-charging



Scanning Electrochemical Microscopy

# Alloy Fabrication Current Capabilities

## NETL-Research and Innovation Capabilities



### Melt Processing Capabilities

- Air Induction Melting: up to 300 lbs
- VIM: 15, 50 and 500 lbs
- Vacuum Arc Remelt/Electro-Slag Remelt 3-to-8-inch diameter ingots

### Thermo-Mechanical Processing Capabilities

- Heat-treatment furnaces: 1650°C, inert atmospheres and controlled cooling.
- Press Forge: 500 Ton
- Roll mills: 2 and 4 high configurations.



# Alloy Fabrication Future Capabilities

## NETL-Research and Innovation Capabilities

### Melt Processing Capabilities

- Alloy Development Research Building, completion in 2026.
- Enhanced melt processing capabilities for high temperature and ultra-high temperature alloys.
- Operational Fall 2026.

### Thermo-Mechanical Processing Capabilities

- Operational in 2025/2026.
- 1500 Ton Press Forge
- 800 Ton Extrusion Press
- Wire Drawing Equipment
  - ★ Experimental wire-based/solid feedstocks for additive manufacturing

### Additive Manufacturing Capabilities

- Operational in 2025
- Lased Direct Energy Deposition Dual Wire/Powder Feed Tool



Good progress towards screening the tensile, creep, and fatigue properties up to 815 °C in air and the native hydrogen embrittlement susceptibility at room temperature.

## Examination of L-PBF superalloy candidates revealed:

- **Microstructure**: Precipitate & carbide phases observed are consistent with conventional alloys after selected heat treatments. L-PBF 625 and 282 show near equiaxed grain structure
  - (1) Fine  $\text{Al}_2\text{O}_3$  oxide inclusions in L-PBF 625, which are highly stable with no noticeable impact on properties
  - (2) Grain boundary stabilization with densely distributed  $\delta$ -precipitates along grain boundaries in L-PBF 718
- **Tensile behavior** is consistent with wrought, particularly L-PBF 282 behavior, while L-PBF 625 & 718 showed modest differences, indicating good potential to apply within IGT.
- **Creep behavior studied (650 – 815 °C / 100 – 600 MPa)**: L-PBF alloys performed consistently with reports for wrought counterparts, with L-PBF 718 on lower end statistically, likely due to refined grain structure.
- **LCF behavior at 650 °C**: S-N curve comparison with literature data looks promising.
- **Hydrogen embrittlement**: As-received L-PBF 625 is the least prone to hydrogen embrittlement, while L-PBF 718 is the most prone